Figure S1

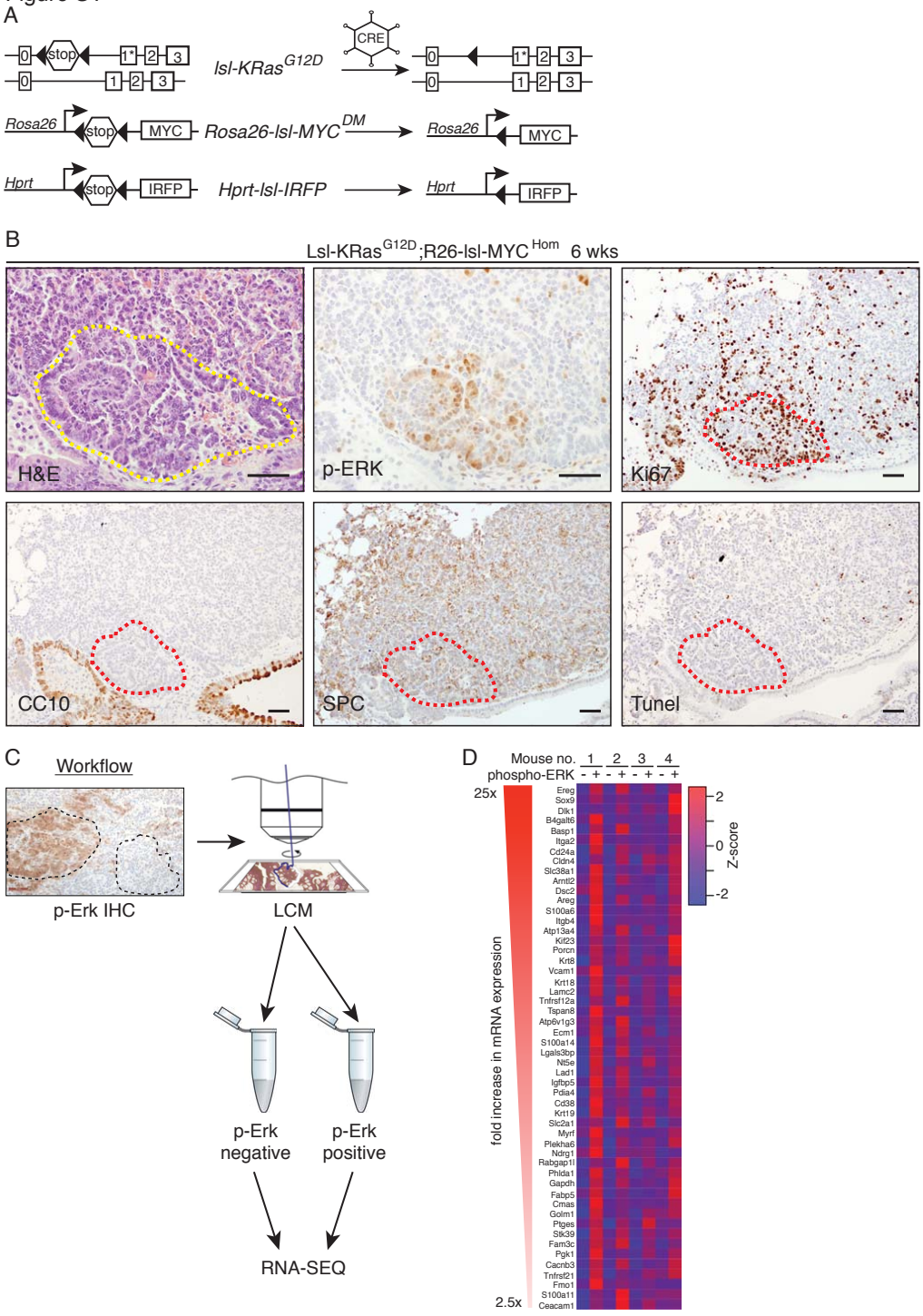
A
stop
lsl-KRas G12D
CRE
Rosa26
MYC
Rosa26-lsl-MYC DM
Hprt
IRFP
Hprt-lsl-IRFP
B
Lsl-KRas G12D;R26-lsl-MYC Hom 6 wks
H&E
p-ERK
Ki67
CC10
SPC
Tunel
C
Workflow
p-Erk IHC
LCM
p-Erk negative
p-Erk positive
RNA-SEQ
D
Mouse no. 1 2 3 4
phospho-ERK - + - + - + - +
25x
2.5x
fold increase in mRNA expression
Z-score
2
0
-2
Ereg
Sox9
Dlk1
B4galt6
Basp1
Itga2
Cd24a
Cldn4
Slc38a1
Arntl2
Dsc2
Areg
S100a6
Itgb4
Atp13a4
Kif23
Porcn
Krt8
Vcam1
Krt18
Lamc2
Tnfrsf12a
Tspan8
Atp6v1g3
Ecm1
S100a14
Lgals3bp
Nt5e
Lad1
Igfbp5
Pdia4
Cd38
Krt19
Slc2a1
Myrf
Plekha6
Ndrg1
Rabgap1l
Phlda1
Gapdh
Fabp5
Cmas
Golm1
Ptges
Stk39
Fam3c
Pgk1
Cacnb3
Tnfrsf21
Fmo1
S100a11
Ceacam1

Supplemental Figures

Figure S1: Characterization of KM lung tumors. Relates to main figures 1, 2 & 3.

A) Schematic of allele activation: Adult (8-10 week old) mice bearing the indicated conditional alleles were administered recombinant Adeno-CRE via intra-nasal installation and maintained for the durations indicated in the text, or until symptomatic. **B)** Serial sections from an lsl-KRas^{G12D};R26-lsl-MYC^{Hom} mouse lung harvested at 6 weeks post induction (PI) and stained with the indicated antibodies or TUNEL stained. Scale bars = 50μM. Images are representative of lungs from at least 5 mice analyzed for each stain. Outline demarcates the approximate p-Erk positive tumour region. **C)** Workflow of laser-capture micro-dissection (LCM) of formalin fixed paraffin-embedded KM lung tumors. Serial sections were first stained for p-Erk expression to identify p-Erk^{High} and p-Erk^{Low} tumor regions. Cresyl violet-stained adjacent sections were then subject to LCM upon identification of the corresponding regions. Messenger RNA was purified from harvested material and analysed by RNA-SEQ. **D)** Heatmap of selected gene expression in p-Erk low (-) and p-Erk high (+) tumors from 4 individual mice, ranked by order of mean fold-increase in expression (range = 24.82 - 2.5). Significantly modulated genes were selected from the RNA-SEQ dataset based on evidence of gene amplification or mRNA overexpression in published human lung cancer datasets, accessed via cBioPortal and Oncomine.

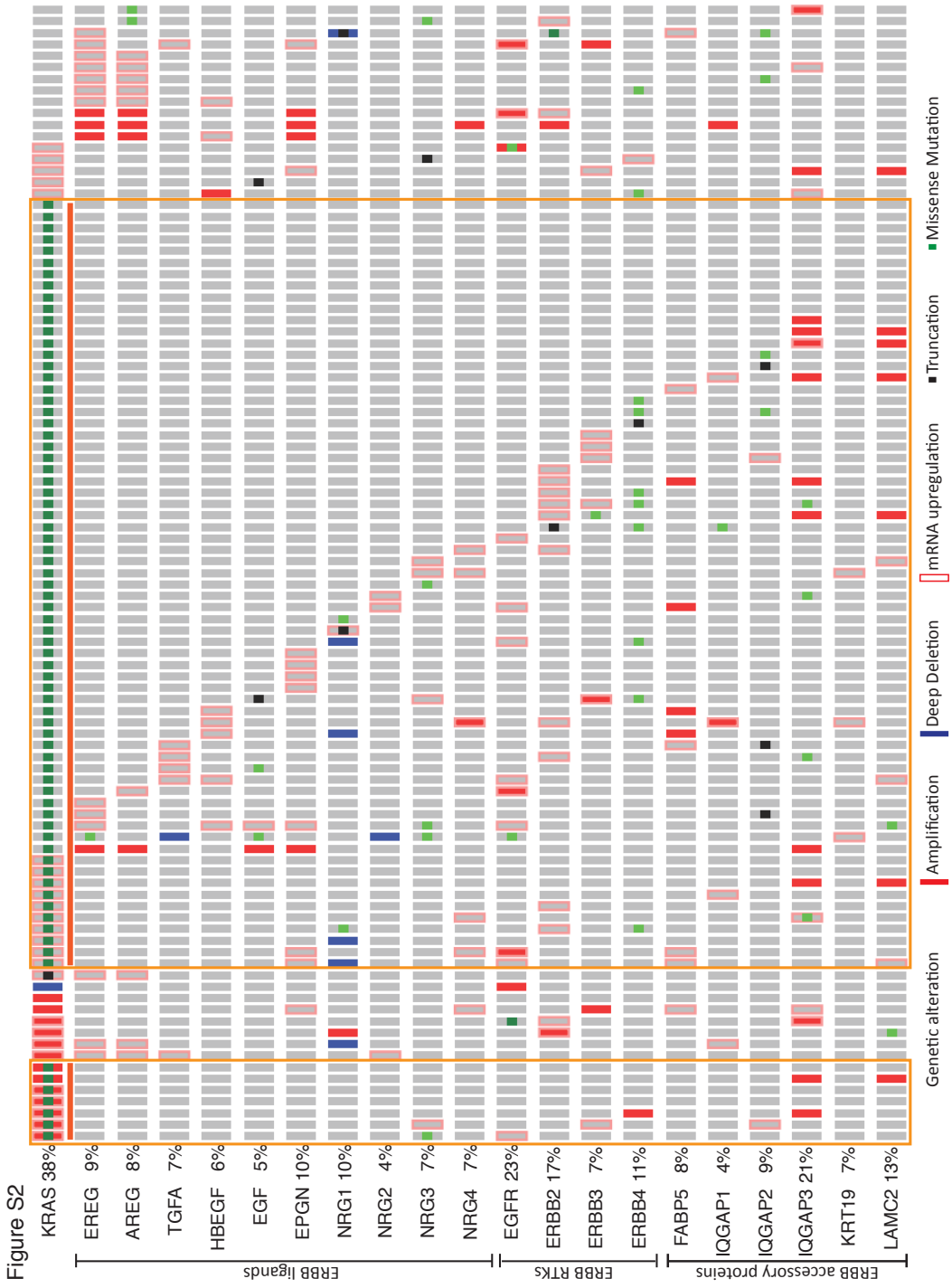
Figure S2
KRAS 38%
EREG 9%
AREG 8%
TGFA 7%
HBEGF 6%
EGF 5%
EPGN 10%
NRG1 10%
NRG2 4%
NRG3 7%
NRG4 7%
EGFR 23%
ERBB2 17%
ERBB3 7%
ERBB4 11%
FABP5 8%
IQGAP1 4%
IQGAP2 9%
IQGAP3 21%
KRT19 7%
LAMC2 13%
ERBB ligands
ERBB RTKs
ERBB accessory proteins
Genetic alteration
Amplification
Deep Deletion
mRNA upregulation
Truncation
Missense Mutation

Figure S2: Genomic alterations and expression data of ERBB network genes in human KRAS mutant Lund Adenocarcinoma. Relates to main figure 3.

Each column represents an individual tumor. Genes are grouped as ERBB ligands, ERBB RTKs and ERBB accessory proteins. Percentages refer to the frequency of alteration across all lung adenocarcinoma. Orange bars (top) emphasize cases of KRAS mutation (N=74, of which 73 are codon 12 mutant) while orange boxes outline the ERBB network in the same cases. Green dots indicate coding alterations; black dots indicate truncation mutations; solid red bars denote gene amplification; open red bars show elevated mRNA expression; solid blue bars indicate deep deletion. Grey bars indicate no detected alteration. Data are derived from the published TCGA Lung Adenocarcinoma cohort as accessed via cBioportal (truncated at the right).

Figure S3

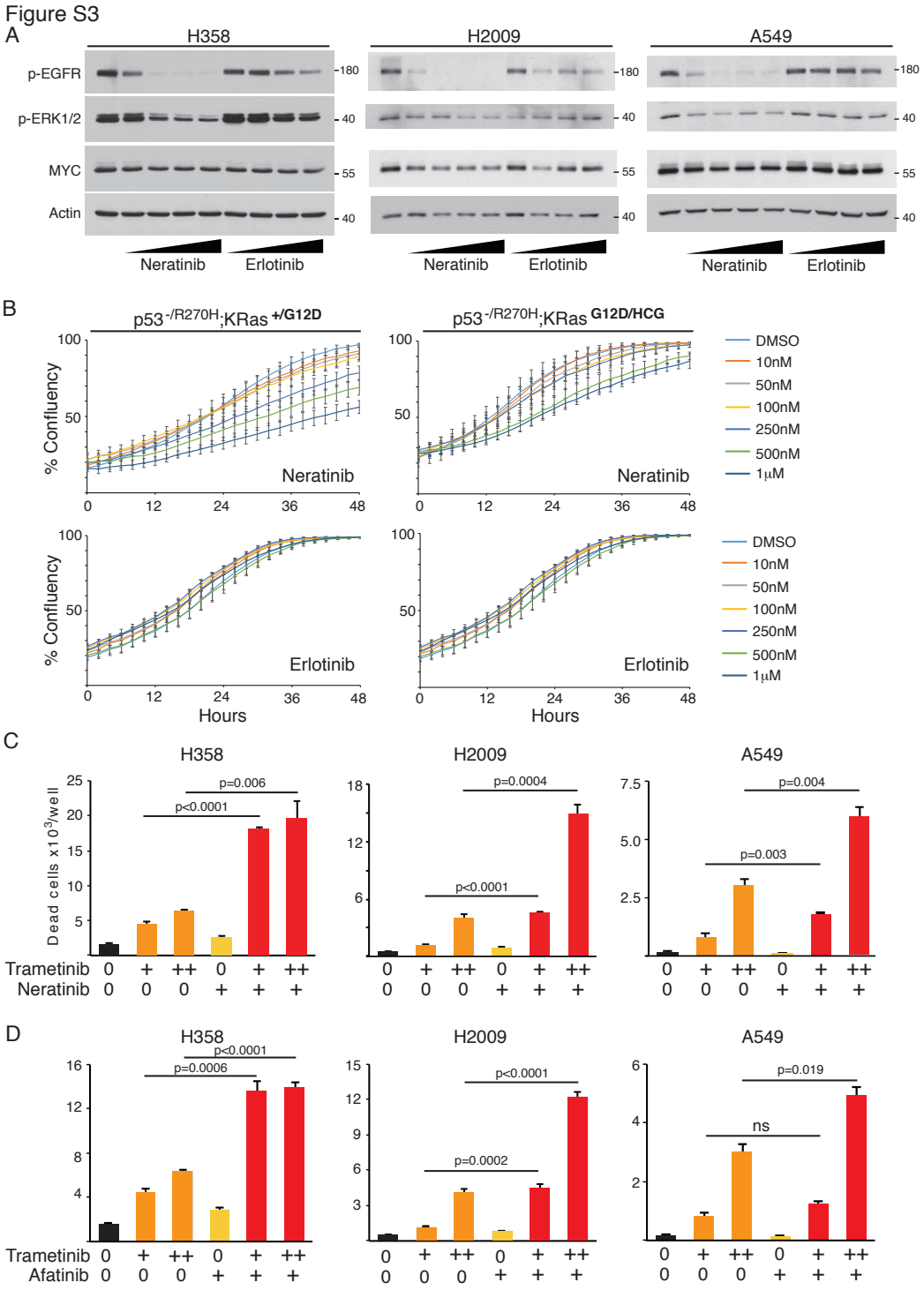
A
H358
H2009
A549
p-EGFR
p-ERK1/2
MYC
Actin
180
40
55
Neratinib
Erlotinib
B
p53-/R270H;KRas +/G12D
p53-/R270H;KRas G12D/HCG
% Confluency
Neratinib
Erlotinib
Hours
DMSO
10nM
50nM
100nM
250nM
500nM
1μM
C
H358
H2009
A549
Dead cells x10^3/well
p=0.006
p<0.0001
p=0.0004
p=0.004
p=0.003
Trametinib
Neratinib
D
H358
H2009
A549
p<0.0001
p=0.0006
p=0.0002
p=0.019
ns
Trametinib
Afatinib

Figure S3: ERBB blockade enhances MEK inhibitor induced NSCLC cell death. Relates to main figures 4 & 5.

A) Lysates from KRAS mutant NSCLC cells treated with increasing doses of Erlotinib or Neratinib were subject to immunoblotting with the indicated antibodies. **B)** Growth curves of $KRas^{G12D/wt}$;$p53^{R270H/-}$ (single copy $KRas^{G12D}$) and $KRas^{G12D/HCG}$;$p53^{R270H/-}$ (high copy gain $KRas^{G12D}$) murine lung tumor lines treated with the indicated doses of Neratinib (upper panels) or Erlotinib (lower panels) and monitored by Incucyte time-lapse. Error bars denote SD of technical triplicates. Data are representative of at least 2 independent experiments. **C)** Quantification of cell death in KRAS mutant human lung cancer lines upon treatment with Neratinib (250nM) alone or in combination with 2 doses (10nM & 100nM) of the MEK inhibitor Trametinib. Mean and SEM of 3 biological replicates from a representative experiment shown. ANOVA followed by Tukey test; ns = not significant. Lower doses of drug were used for H358 cells (50nM Neratinib and 50nM Trametinib) due to their greater sensitivity to either drug alone. **D)** Quantification of cell death in KRAS mutant human lung cancer lines upon treatment with Afatinib (1μM) alone or in combination with 2 doses (10nM & 100nM) of the MEK inhibitor Trametinib. Mean and SEM of 3 biological replicates from a representative experiment shown. ANOVA followed by Tukey test; ns = not significant. Lower doses of drug were used for H358 cells (50nM Afatinib and 50nM Trametinib) due to their greater sensitivity to either drug alone.

Figure S4

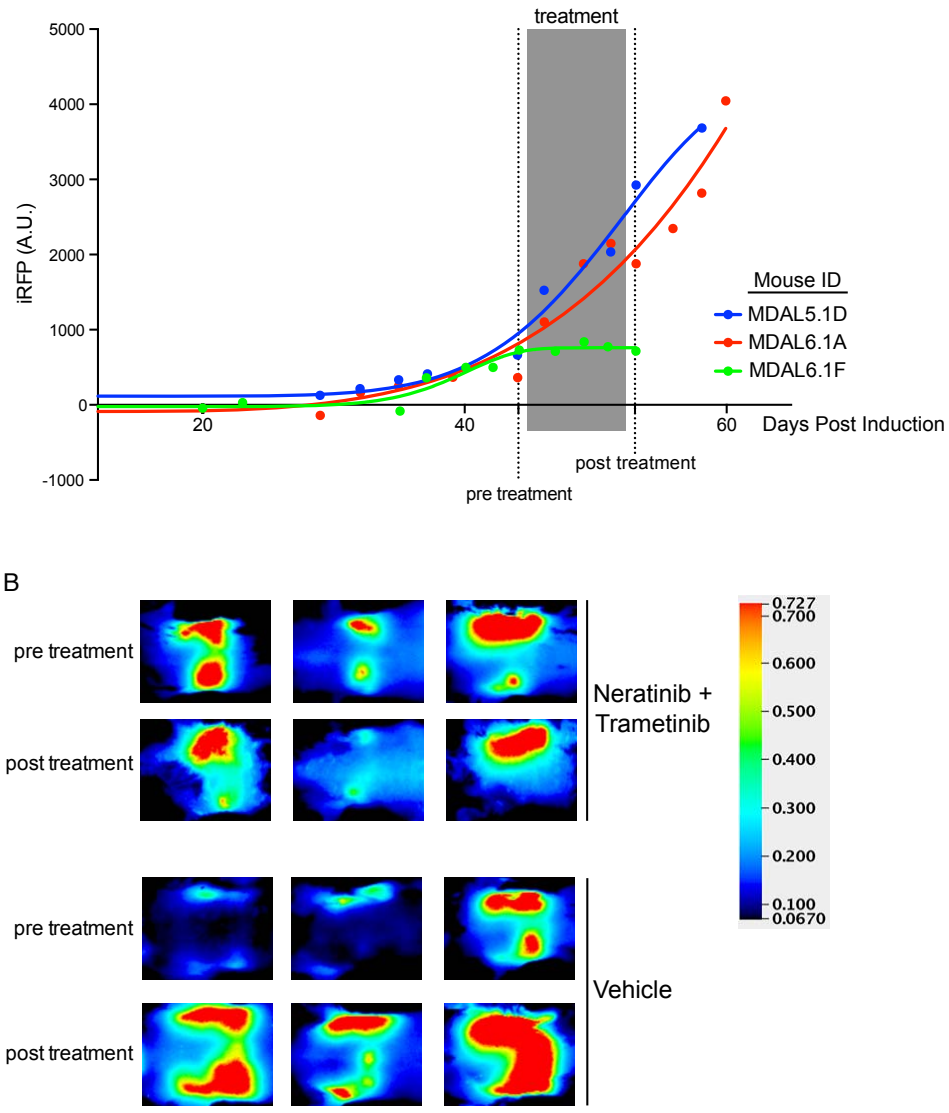
A
treatment
5000
4000
3000
2000
1000
0
-1000
iRFP (A.U.)
20
40
60
Days Post Induction
post treatment
pre treatment
Mouse ID
MDAL5.1D
MDAL6.1A
MDAL6.1F
B
pre treatment
post treatment
Neratinib +
Trametinib
pre treatment
post treatment
Vehicle
0.727
0.700
0.600
0.500
0.400
0.300
0.200
0.100
0.0670

Figure S4: Longitudinal in-vivo imaging of nascent lung tumors. Relates to main figure 5.

A) KM mice were interbred with *Hprt-lsl-iRFP*, induced with Adeno-CRE as before, and monitored for tumor growth using a Licor PEARL imager. Circles indicate days of imaging. Data are normalized to background fluorescence for each mouse, set to 0, and signal intensity curves were calculated using the Weibull growth equation. Upon consistent detection of pulmonary fluorescence, mice were administered the combination of Neratinib + Trametinib (MDAL6.1F), or vehicle control (MDAL5.1D & 6.1A) for 1 week (grey bar). The presence of tumors was confirmed upon sacrifice. **B)** Representative images of mice as from (A) showing fluorescent detection of iRFP-labeled KM tumors before and after drug (upper panels) or vehicle (lower panels) treatment. The same colorimetric scale was used for each image. Pre- and post-treatment images, separated by 9 days, are shown for each mouse.

Table S1

Modulated during progression to p-Erk + tumors			Modulated by Neratinib *in vitro*					
			H358		H2009		A549	
Pathway	Rank	FDR	Rank	FDR	Rank	FDR	Rank	FDR
Cytoskeletal remodeling, TGF, WNT pathways	1	1.7e-24	1	2.7e-26	1	1.5e-26	1	2.3e-27
Cytoskeletal remodeling	2	9.0e-23	2	3.2e-21	2	2.1e-22	4	2.4e-22
Transport - Clathrin-coated vescicle cycle	3	3.6e-19	3	2.5e-18	3	2.2e-21	2	1.4e-22
Apoptosis & survival, NGF/TrkA PI3K signaling	4	1.4e-15	4	4.4e-17	4	7.8e-19	3	1.6e-22
Transcription, Sin3 & NuRD regulated	5	1.6e-15	8	4.9e-16	6	4.1e-17	6	4.9e-18
Immune Response, IL4 signaling	6	9.1e-15	19	2.6e-13	14	6.6e-15	8	7.1e-17
Cell Cycle, influence of Ras & Rho in G1/S	7	2.7e-14	11	7.8e-15	8	5.2e-16	7	5.8e-17
Cell Adhesion, Chemokines & adhesion	8	2.8e-14	7	2.3e-16	17	1.5e-14	19	1.1e-13
Development, TGF-beta receptor signaling	10	2.3e-13	6	2.1e-16	5	1.2e-17	13	1.2e-14
Translation, regulation of EIF4F activity	11	3.2e-13	14	1.1e-13	13	6.6e-15	14	1.2e-14
Development, EGFR signaling	12	4.4e-13	12	1.9e-14	10	6.7e-16	11	4.3e-15
Receptor mediated axon growth repulsion	13	5.4e-13	26	3.0e-12	21	3.0e-13	10	3.4e-15
Androgen receptor activation	14	5.6e-13	5	7.6e-17	16	1.1e-14	15	1.2e-14
Epigenetic regulation of gene expression	16	1.6e-12	21	5.6e-13	22	3.4e-13	16	5.0e-14
IGF family signlaing in colorectal cancer	17	1.6e-12	22	5.6e-13	18	3.2e-14	29	2.2e-12
TGFb-dependent induction of EMT via MAPK	18	1.6e-12	31	7.6e-12	25	7.4e-13	26	1.6e-12
NGF/TrkA MAPK-mediated signaling	19	2.1e-12	9	1.3e-15	9	6.7e-16	9	9.0e-16
Regulation of STK3/4 (Hippo) and YAP/TAZ	20	2.9e-12	18	2.6e-13	15	1.1e-14	12	9.4e-15

Table S1: Summary of Metacore GeneGO pathway analysis. Relates to main figure 4.

The blue shaded region demarcates pathways modulated as KM tumours progress to $pErk^{High}$ expression, ranked by false discovery rate (FDR). The mauve shaded region indicates the Rank and FDR of the same pathways upon treatment of the indicated KRAS mutant human NSCLC cell lines with Neratinib.